

Equivalent width, shape and proper motion of the iron fluorescent line emission from the molecular clouds as an indicator of the illuminating source X-ray flux history

R. Sunyaev,^{1,2} E. Churazov,^{1,2}

¹ *MPI fur Astrophysik, Karl-Schwarzschild-Strasse 1, 85740 Garching, Germany*

² *Space Research Institute (IKI), Profsovnaya 84/32, Moscow 117810, Russia*

To appear in MNRAS

ABSTRACT

Observations of the diffuse emission in the 8–22 keV energy range, elongated parallel to the Galactic plane (Sunyaev et al. 1993) and detection of the strong 6.4 keV fluorescent line with ~ 1 keV equivalent width from some giant molecular clouds (e.g. Sgr B2) in the Galactic Centre region (Koyama 1994) suggest that the neutral matter of these clouds is (or was) illuminated by powerful X-ray radiation, which gave rise to the reprocessed radiation. The source of this radiation remains unknown. Transient source close to the Sgr B2 cloud or short outburst of the X-ray emission from supermassive black hole at the Galactic Centre are the two prime candidates under consideration. We argue that new generation of X-ray telescopes combining very high sensitivity and excellent energy and angular resolutions would be able to discriminate between these two possibilities studying time dependent changes of the morphology of the surface brightness distribution, the equivalent width and the shape of the fluorescent line in the Sgr B2 and other molecular clouds in the region. We note also that detection of broad and complex structures near the 6.4 keV line in the spectra of distant AGNs, which are X-ray weak now, may prove the presence of violent activity of the central engines of these objects in the past. Accurate measurements of the line shape may provide an information on the time elapsed since the outburst. Proper motion (super or subluminal) of the fluorescent radiation wave front can give additional information on the location of the source. Observations of the described effects can provide unique information on the matter distribution inside Sgr B2 and other giant molecular clouds.

Key words: line: formation – X-rays: general – ISM: individual: SGR B – Galaxy: centre.

1 INTRODUCTION

Prediction (Sunyaev et al. 1993) and discovery (Koyama 1994; Koyama et al. 1996) of the bright iron fluorescent K_α line in the direction of the molecular cloud Sgr B2 and Radio Arc in the Galactic Centre region should not remain unnoticed by the astrophysicists planning in the nearest future launch of the sensitive X-ray spectrometers on board *AXAF*, *XMM*, *ASTRO-E*, *ABRIXAS*, *Spectrum-X-Gamma*. These spectrometers will provide high angular resolution from seconds to minutes of arc and spectral resolution from 5 to 140 eV near X-Ray lines of iron in the 6–7 keV energy band. The missions of the next millennium, starting with *Constellation* (White, Tananbaum & Kahn, 1997) and *XEUS* (Turner et al. 1997), are to achieve energy resolution of 2 eV and better. Particularly relevant problem, which deserves further consideration, is the illumination of a molecular hydrogen cloud with column density

$N_H \sim 10^{23} - 10^{24} \text{ cm}^{-2}$ (i.e. $\tau_T \sim 0.1 - 1$) by a variable X-ray emission from a bright transient source inside the cloud or outside the cloud (e.g. short episode of the effective accretion onto Sgr A* due to the tidal star disruption). The solution of this problem allows one to study the time evolution of the spectrum emerging from the cloud after fading of the primary X-ray source. The radius of the Sgr B2 cloud is of the order of 20 pc (e.g. Lis & Goldsmith 1989), although the size of the dense core(s) is significantly smaller (~ 0.3 pc, e.g. de Vicente et al. 1997). Depending on the mutual location of the cloud and a primary source of the continuum emission substantial evolution of the morphology, flux, equivalent width and shape of the iron fluorescent line might be noticed on the time scale as short as 0.1–10 years (the value which is not incomparable with the life time of the best modern space observatories). Three years already passed since the moment of the first firm detection of the line

from Sgr B2 (Koyama 1994; Koyama et al. 1996). Detailed observations would allow one to reveal the geometry of the problem (i.e. mutual location of the primary source and the cloud), time elapsed since fading of the primary source flux. Observations might also shed additional light on the mass of the cloud, its uniformity and, provided energy resolution better than 1 eV, on the matter and velocity distribution inside the cloud.

As the first approximation we are considering below qualitatively how the effects of time delay, large opacity and scattering by bound electrons affect the appearance of the 6.4 keV line from a molecular cloud illuminated by a continuum X-ray emission. Throughout the paper we adopted the approximation of Morrison and McCammon (1983) for photoelectric absorption ($\sigma_{ph}(E)$) in the neutral gas, having a normal abundance of heavy elements, an abundance of iron of $\delta_{Fe} = 3.3 \times 10^{-5}$ with respect to hydrogen, a cross section of photoabsorption from iron K-shell as $\sigma_{Fe}(E) = 3.53 \times 10^{-20} \times (E/7.1 \text{ keV})^{-3} \text{ cm}^2/\text{atom}$ and a K_α fluorescent yield $Y = 0.3$ (e.g. Bambinek et al., 1972). For simplicity we are considering (unless stated otherwise) the simplest case of a point source of continuum X-ray emission in the centre of a spherically symmetric cloud of neutral gas.

The formation of the K_α line from the neutral matter illuminated by a continuum radiation was considered in many publications (e.g. Basko, Sunyaev & Titarchuk 1974, Fabian 1977, Basko 1978, Vainshtein & Sunyaev 1980, Inoue 1985, George & Fabian 1991, Matt et al. 1991, Awaki et al. 1991, Nandra & George 1994, Ghisellini et al. 1994). In the discussion below we present the arguments which are particularly relevant to the observations of the Galactic Centre region in the neutral iron fluorescent line.

This paper does not pretend to explain the nature of an X-ray emission from the Galactic Centre region. Instead we consider a number of simple effects which might play an important role in the environment like the central region of our Galaxy. These effects could be used by the missions like *Constellation* and *XEUS* to verify the hypothesis that molecular clouds near the Galactic Centre were exposed to outburst of hard X-ray radiation:

- Dependence of the morphology of the 6.4 keV surface brightness distribution on the mutual location of the source and the cloud.
- Apparent motion (sub or superluminal) of the features associated with propagation of the source radiation through the clouds.
- Evolution of equivalent width and shape of the 6.4 keV line as an indicator of multiple scatterings and time elapsed since outburst.

The structure of the paper is as follows: in sections 2 and 3 we discuss temporal behavior of scattered flux and morphology of the scattered radiation associated with first scattering, in the subsequent sections 4–7 we argue that equivalent width and the shape of the fluorescent line (due to multiple scatterings) may be used as another indicator of cloud illumination with powerful flares in the past, section 8 summarizes the results. In appendix a simplified derivation of the evolution of the equivalent width and shape of the line after multiple scatterings is given.

2 THE LUMINOSITY OF ILLUMINATING SOURCE

Observations of the Galactic Centre region with the GRANAT/ART-P telescope revealed a diffuse component above ~ 8 keV elongated parallel to the Galactic plane and resembling the distribution of the molecular gas clouds (Sunyaev et al. 1993; Markevitch, Sunyaev & Pavlinsky 1993). It was suggested that this component is due to the Thomson scattering by dense molecular gas of the X-rays from nearby compact sources and as a consequence existence of bright K_α iron fluorescent line was proposed. Further evidence in support of this assumption came from ASCA observations of this region, which revealed strong 6.4 keV line flux from the general direction of the largest molecular complexes (e.g. Koyama, 1994). The Sgr B2 complex was found to be especially bright in the 6.4 keV line, at the level of $1.7 \cdot 10^{-4} \text{ photon s}^{-1} \text{ cm}^{-2}$ (Koyama et al. 1996). Such a high flux in the fluorescent line requires a powerful source of primary X-ray emission which gives rise to the reprocessed radiation. Since the light crossing time of the Galactic Centre region is as long as several hundred years, observed reprocessed radiation may be associated with the source which is dim at present, but was very bright some hundred years ago. Such a scenario has been suggested by Sunyaev, Markevitch & Pavlinsky (1993) and Koyama (1994), Koyama et al. (1996), the Galactic Centre (i.e. Sgr A*) itself being the primary candidate. Given the distance from the Sgr B2 complex to the GC ($\sim 40'$ or about 100 pc in projection) Sunyaev, Markevitch & Pavlinsky (1993) and Koyama et al. (1996) estimated the luminosity of the putative GC source in excess of $10^{39} \text{ erg s}^{-1}$ some hundred years ago. The flux in the 6.4 keV line from the cloud exposed to the continuum radiation is given by the expression:

$$F_{6.4} = \frac{\Omega}{4\pi D^2} n_{Fe} r Y \int_{7.1}^{\infty} I(E) \sigma_{ph}(E) dE \quad \text{phot s}^{-1} \text{ cm}^{-2} \quad (1)$$

where Ω is the solid angle of the cloud from the location of the primary source, D is the distance to the observer, $n_{Fe} r$ is iron column density of the cloud, $I(E)$ is the photon spectrum of the primary source ($\text{phot s}^{-1} \text{ keV}^{-1}$). Since $\sigma_{ph}(E)$ is a steep function of energy the 6.4 keV flux depends mainly on the source flux at ~ 7 –9 keV. It is convenient therefore to express 6.4 keV flux through the source flux at 8 keV:

$$F_{6.4} = \phi \frac{\Omega}{4\pi D^2} \frac{\delta_{Fe}}{3.3 \times 10^{-5}} \tau_T I(8 \text{ keV}) \quad \text{phot s}^{-1} \text{ cm}^{-2} \quad (2)$$

where ϕ is a factor of the order of unity, which depends (weakly) on the shape of the source spectrum. For the bremsstrahlung spectrum factor ϕ varies from 1 to 1.3 when temperature is varying from 5 to 150 keV. For convenience one can replace $I(8)$ in the above expression by the measure of the continuum source luminosity at 8 keV in the 8 keV wide energy band: $L_8 = I(8) \times 8 \times 8 \times 1.6 \cdot 10^{-9} \text{ erg s}^{-1}$.

$$F_{6.4} = \phi 10^7 \frac{\Omega}{4\pi D^2} \frac{\delta_{Fe}}{3.3 \times 10^{-5}} \tau_T L_8 \quad \text{phot s}^{-1} \text{ cm}^{-2} \quad (3)$$

The value of L_8 characterizes the luminosity of the source in standard X-ray band. E.g. for bremsstrahlung spectra with temperatures from 5 up to 150 keV L_8 corresponds to ≈ 40 –45 per cent of the source luminosity in the 1–20 keV band. Thus the luminosity of the source required to produce

observed 6.4 keV flux is:

$$L_8 \approx 6 \cdot 10^{38} \times \left(\frac{F_{6.4}}{10^{-4}}\right) \times \left(\frac{0.1}{\tau_T}\right) \times \left(\frac{\delta_{Fe}}{3.3 \times 10^{-5}}\right)^{-1} \times \left(\frac{R}{100 \text{ pc}}\right)^2 \quad (4)$$

where R is the distance from the source to the cloud. The above crude estimate assumes that the source is well outside the cloud, which has diameter of ~ 14 pc (Koyama et al. 1996) and $\tau_T \ll 1$. Although high enough this value is still much below the Eddington limit of $\sim 10^{44} \text{ erg s}^{-1}$ for the $\sim 10^6 M_\odot$ black hole (Genzel et al. 1994) and even rather short (e.g. several days) flare at the Eddington level could provide the required flux. Note that if the duration of the flare is shorter than the light crossing time of the cloud the above estimate should be multiplied by a factor roughly $\frac{r/c}{\Delta t}$, where r/c is the light crossing time of the cloud and Δt is the duration of the flare. In other words for very short flare the product $L \times \Delta t$ (i.e. luminosity \times duration) defines the 6.4 keV flux (Sunyaev et al. 1993). A less energetic object is required if one assumes that the primary source of continuum emission is located in the vicinity of the Sgr B2 complex (or even inside it). For the source embedded into the uniform cloud the luminosity is only:

$$L_8 \sim 6 \cdot 10^{35} \times \left(\frac{F_{6.4}}{10^{-4}}\right) \times \left(\frac{0.1}{\tau_T}\right) \times \left(\frac{\delta_{Fe}}{3.3 \times 10^{-5}}\right)^{-1} \quad (5)$$

For hard spectra (e.g. bremsstrahlung with $kT \sim 100$ keV) the 1–150 keV luminosity is factor of ~ 7 larger than L_8 , but it is still well consistent with observed luminosities of X-ray Novae with hard spectra. This estimate should also be increased if the source was bright during period of time shorter than the light crossing time of the cloud.

In the presence of the steady primary source inside the cloud the expected equivalent width of the 6.4 keV line (with respect to the primary continuum flux) EW is about $1 \times \tau_T$ keV, where τ_T is the Thomson depth of the medium, surrounding the source. If the primary source radiation diminishes (or if the source is outside the region over which the spectrum is collected), then the equivalent width is equal to ~ 1 keV (e.g. Fabian 1977, Vainshtein & Sunyaev 1980) – the value, which is rather insensitive to the cloud parameters like Thomson optical depth (as long as it is low enough) or particular distribution of scattering matter. This happens because both 6.4 keV and scattered continuum fluxes are proportional to the optical depth of the cloud and intensity of the primary radiation. In particular case of the Sgr B2 cloud the equivalent width of the observed line is of the order of 1 keV (Koyama et al. 1996), suggesting that observed spectrum is dominated by scattered radiation. Provided that the cloud is optically thin and abundance of iron is $\sim 3.3 \times 10^{-5}$ then large value of the equivalent width immediately excludes the possibility that steady source of continuum radiation is located inside the cloud or is projected onto the cloud. The hypothesis that hot plasma surrounding the cloud is responsible for primary radiation can be rejected for the same reason even without knowledge of its luminosity. Furthermore assuming again that the source is steady and has hard ($T_e = 150$ keV) bremsstrahlung spectrum then one would expect the source to be seen in the GRANAT/SIGMA observations. Indeed for given source spectrum one can estimate 35–100 keV luminosity of the source from equation

(5): $L_{hard} \sim 3 \cdot 10^{36} \times \left(\frac{0.1}{\tau_T}\right) \times \left(\frac{\delta_{Fe}}{3.3 \times 10^{-5}}\right)^{-1} \text{ erg s}^{-1}$. Actual conservative upper limit is at least factor of 5 lower (see Gilfanov & Sunyaev, 1998).

Another possibility is that X-ray emission of the Sgr B2 cloud is produced by a number of steady sources (may be diffuse) spreaded across the cloud. At each particular energy only regions which are screened from us by an absorbing depth of $\tau_{ph}(E) \leq 1$ will contribute to the emergent flux. As long as line of sight depths to different emitting regions spans wide range of values, ‘flat’ continuum spectrum, like observed from Sgr B2 (Koyama et al. 1996), can be formed. Observationally the spectrum of such a cloud might resemble the reflected spectrum, usually considered in application to AGNs or X-ray binaries. However, in order to provide large equivalent width of the 6.4 keV line, most of the emitting regions should be screened from us by a hydrogen column of few 10^{24} cm^{-2} . In this case (as discussed further in section 4) continuum photons at ~ 6 keV will be absorbed, while photons with higher energies (e.g. 10–20 keV) may reach periphery of the cloud and produce 6.4 keV photons. The total luminosity of such a cloud (after correction for absorption) should be considerably larger than that given by expression (5).

The constraints on the source luminosity can be drastically reduced if we assume that the emission of the primary source is intrinsically strongly collimated. This is particularly important when considering Sgr A* as a potential source of powering the 6.4 keV line emission from Sgr B2. The solid angle of the Sgr B2 cloud as from the Sgr A* position is of the order or less than ~ 0.02 str. Therefore required flux from Sgr A* (within the narrow cone) is only of the order of $L_8 \sim 10^{36} \text{ erg s}^{-1}$ i.e. almost 3 orders of magnitude lower than that given by expression (4). We note that this value places an absolute lower limit on the luminosity of Sgr A* as a potential source for powering Sgr B2 cloud. The brightness of the Sgr B2 cloud would then be explained by the location of the cloud within this narrow cone of the Sgr A* emission. If this hypothesis is correct, than high angular resolution observations could perhaps find evidence of the ‘jet-like’ structures formed by the Thomson scattering (as discussed by Gilfanov, Sunyaev & Churazov 1987) by the molecular gas within the cone of the emission.

Another hypothesis of a similar kind is that we deal with obscured AGN, i.e. that Sgr A* is a very bright steady X-ray source (with luminosity as it follows from expression (4)), but cold matter (at least $N_H \sim 10^{25} \text{ cm}^{-2}$) in the very vicinity of the source blocks our line of sight (see e.g. Predehl & Trümper 1994), while Sgr B2 is exposed to the Sgr A* emission (Koyama et al. 1996). The commonly accepted value for interstellar extinction towards the brightest IR stars near the Galactic Centre is $A_v \sim 31$ (Rieke, Rieke & Paul 1989), which corresponds to hydrogen column density of $N_H \sim 6 \cdot 10^{22} \text{ cm}^{-2}$ i.e. at least two orders of magnitude lower, than required. Absorption by the partly ionized gas in the shell surrounding Sgr A* is also low (Beckert et al. 1996). It is possible, however, that the edge of the inner accretion disk obscures our line of sight. The major problem with this hypothesis (see e.g. Koyama et al., 1996) is the lack of bright infrared source at the location of Sgr A* (Menten et al. 1997).

Thus there is no obvious candidate for the source of primary radiation which present day brightness is sufficient

to power 6.4 keV emission from Sgr B2 cloud. We therefore consider below the situation when the source of continuum radiation is variable and it is now in the weak state. One can consider two different possibilities for the location of such a source:

A The primary (transient) source was located inside (or very close) to the Sgr B2 cloud.

B The primary radiation is due to intense emission from Sgr A* in the past.

In any case the emission of the source is variable and perhaps on the time scales shorter than light crossing time of the cloud. E.g. for typical X-ray Nova flux is falling down with e-folding time of the order of 40 days (e.g. Tanaka & Shibazaki, 1996), while the rising time can be as short as one or few days. For the transient accretion event onto Sgr A* (e.g. capture of tidally disrupted star) we also might expect a flare duration at a time scale of years (Rees 1988). Thus the observed picture may not be static and some information can be obtained studying its time evolution.

3 TIME DEPENDENT FLUX, MORPHOLOGY (BRIGHT SPOTS) AND PROPER MOTION OF THE 6.4 KEV LINE EMITTING REGIONS

3.1 Single scattering problem

Let us consider first the situation when the cloud is illuminated with the relatively short flare. The geometry of the problem is schematically shown in Fig.1. For the short flare surface of the parabola denotes the positions with similar propagation times from the source to the cloud and then to the (distant) observer. The surface ($z/c = (t^2 - (x/c)^2)/2t$) has of course rotational symmetry over the Z axis. Similar time/geometry problem appears in many situations, e.g. while considering scattering of the emission from central source by the electrons in hot intergalactic media (Gilfanov, Sunyaev, Churazov 1987), light echo from supernovae (e.g. Chevalier, 1986) or even as an alternative to the gravitational lensing arcs (Katz 1987; Milgrom 1987). In connection with Sgr B2 which one can make a number of predictions based on such a picture.

3.1.1 Bright spots

If the flare is very short (much shorter than the light crossing time of the cloud) then observed surface brightness at a given moment will be determined not by the total optical depth of the cloud, but rather by the density of the cloud at the surface of the parabola. The parabola ‘scans’ the density profile of the cloud. The surface brightness is defined by the integral $\int \frac{I}{4\pi r^2} ndl$ over the line of sight. The integration limits are defined by two parabolas corresponding to the beginning and the end of the flare. One can write a simple expression for the surface brightness (flux from the solid angle $d\Omega$) of the 6.4 keV line emission:

$$S = 7 \cdot 10^{-6} \left(\frac{n}{10^5 \text{ cm}^{-3}} \right) \left(\frac{\Delta t}{1 \text{ year}} \right) \left(\frac{L_8}{10^{39}} \right) \left(\frac{100 \text{ pc}}{x} \right)^2 \times$$

$$\times \left(\frac{d\Omega}{(15'')^2} \right) \frac{\eta^2}{(1 + \eta^2)} \text{ phot s}^{-1} \text{ cm}^{-2} \quad (6)$$

where Δt is the duration of flare, $\eta = x/ct$, x is the projected distance from the source to the bright spot, t is the time elapsed since the flare. The above formula (scaled to the angular resolutions of the *XMM* and *JET-X* on *Spectrum-X-Gamma*) shows that with integration time of 10^5 seconds and with effective area from ~ 300 to 3000 cm^2 at 6.4 keV these instruments will be able to trace the density variations in the cloud. The estimated size of dense condensations in the Sgr B2 cloud of $\sim 0.5\text{--}0.3 \text{ pc}$ (e.g. de Vicente et al., 1997) is well matched with the angular resolution of these telescopes. Note that for search of the bright spots energy resolution of typical CCD is sufficient. Thus if the Sgr B2 cloud was indeed illuminated by the short flare, then one can expect very strong variations (up to three orders of magnitude according to the data on molecular lines tracers of high density) of the surface brightness of the 6.4 keV flux across the cloud image on the angular scales, corresponding to the size of the nonuniformities in the cloud (i.e. $10\text{--}20''$). If on the contrary the flare was sufficiently extended in time, then surface brightness distribution will reflect total optical depth of the cloud (at a given line of sight), which should be much smoother since contribution to the total scattering mass from extended envelopes dominates.

3.1.2 Superluminal proper motion of the front

Note that with time the position of the parabola will change and the velocity of this change strongly depends on the mutual location of the source and the cloud. In particularly ‘expansion’ velocity of the parabola (Fig.1) over X coordinate (at fixed Z) is $|\dot{x}/c| = 1 + \frac{(ct-x)^2}{2ct|x|}$, i.e. $1 \leq |\dot{x}/c| < \infty$. Therefore it is equal or larger than speed of light for any position. Similarly the velocity of parabola expansion over Z coordinate (at fixed X) is $\dot{z}/c = 1 - \frac{z}{ct} = 0.5 + \frac{x^2}{2(ct)^2}$ ($1/2 \leq \dot{z}/c < \infty$). Note that $\dot{z} < c$ if $z > 0$ (the cloud is behind the source) and $\dot{z} > c$ if $z < 0$ (the cloud is in front of the source). Thus if the cloud is located closer to the observer than the source of the flare, then the whole cloud will be ‘scanned’ much quicker than the light crossing time of the cloud. For the cloud behind the source time evolution will be slowest. Stark et al. (1991) argue that since the radial velocity of the Sgr B2 cloud relative to the GC is only $\sim 40 \text{ km s}^{-1}$ the assumption that it is on the circular orbit at $\sim 180 \text{ km s}^{-1}$ would place it $\approx 400 \text{ pc}$ closer (or further away) from the observer than the Galactic Centre. It is clear that in the case of short flare time dependent effects will be very different for these two cases: for the nearer location one can expect higher flux and much more rapid evolution. If on the contrary the flare was very long (such that the whole cloud is filled with photons), then these two cases will be virtually indistinguishable from each other. However, taking into account that photoabsorption may significantly affect the morphology (especially for dense cores, having considerable depth) it might be possible to discriminate between these two cases.

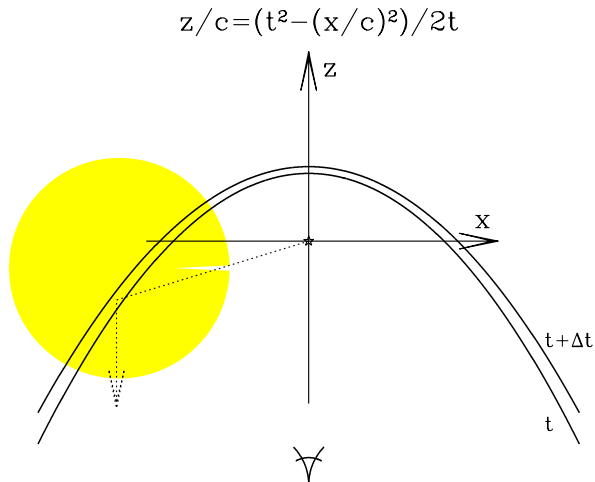


Figure 1. Each point at the surface of the parabola $z/c = \frac{t^2 - (x/c)^2}{2t}$ has similar delay t in propagation time from the source (marked with asterisk) to the scattering place and then to the observer. In the case of a short flare the fluorescent photons which are observed at a given moment of time are produced in the neutral matter located at the surface of the parabola. For a steady source which faded at a given moment of time the exterior of the parabola is filled with primary continuum photons.

3.1.3 Surface brightness distribution (steady source and long flare)

Shown in the Fig.2 (bottom row of images) is the expected surface brightness distribution of the spherically symmetric cloud exposed to steady continuum radiation calculated for different positions of the primary source. We assume here that density of hydrogen molecules in the cloud has the following radial distribution:

$$n(r) = 2.2 \cdot 10^3 + \frac{7.7 \cdot 10^4}{1 + \left(\frac{r}{1.25 \text{ pc}}\right)^2} \text{ cm}^{-3}, \quad r < 22.5 \text{ pc} \quad (7)$$

This distribution closely resembles the model distribution derived by Lis & Goldsmith (1989), although actual density distribution in the Sgr B2 complex is of course much more complex (e.g. Hasegawa et al. 1994, de Vicente et al. 1997). The surface brightness was estimated integrating over the line of sight the product of the gas density in the cloud and radiation field density (which for steady source is $\frac{I_0}{4\pi r^2}$, where I_0 is the intensity of the compact source and r is the distance from the source). Photoabsorption and Thomson scattering were taken into account. The position of the centre of the cloud with respect to the primary source (in the plane defined by the cloud, source and observed as shown in Fig.1) is indicated by the pair of numbers at the bottom of the Fig.2. E.g. (0;0) corresponds to the source at the centre of the cloud; (-100;200) corresponds to the cloud which is shifted by 100 pc to the left from the source and

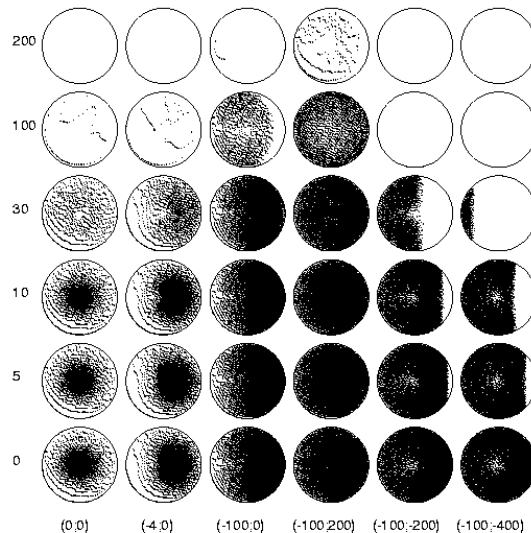


Figure 2. Morphology of the 6.4 keV line surface brightness distribution as a function of time and relative position of the scattering cloud and the compact source of continuum radiation. Time evolution assumes steady source of continuum emission which faded at some moment of time. The time tags marked in the left column indicate the time (in years) elapsed since the moment, when the surface of the parabola (which exterior is filled by primary radiation) touched the cloud for the first time (see text and Fig.1). The position of the cloud with respect to the compact source is indicated with a pair of numbers (in parsecs) at the bottom of the figure. The radius of the cloud was assumed to be 22.5 pc and density distribution according to expression (7).

is located 200 pc further away from the observer than the source. Other rows in Fig.2 show time evolution of the surface brightness morphology, assuming steady source of continuum emission which faded at some moment of time. The time tags marked in the left column indicate the time elapsed since the moment, when the surface of the parabola (which exterior is filled by primary radiation) touched the cloud for the first time. The situation (A) (source inside the cloud) is characterized by a distinct peak in the surface brightness distribution. This peak is simply due to the higher density of the primary radiation close to the source ($I \propto \frac{I_0}{4\pi r^2}$). For the source, located at a large distance from the cloud (compared to the radius of the cloud) surface brightness is much more uniform and reflects roughly Thomson depth of the cloud on the line of sight. Photoabsorption and Thomson scattering cause additional asymmetry – the side of the cloud exposed to the radiation should be brighter. As pointed out by Koyama et al. (1996) the side of the Sgr B2 cloud towards Sgr A* is somewhat brighter, perhaps suggesting that the primary source is at least in general direction of Sgr A*.

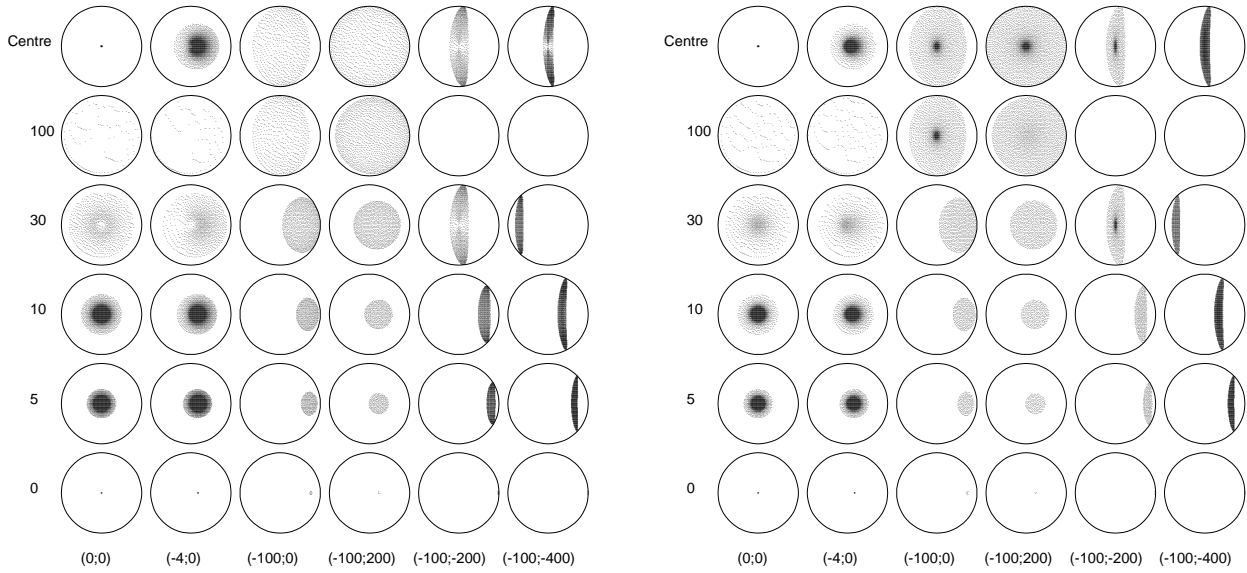


Figure 3. **Left:** Morphology of the 6.4 keV line surface brightness distribution as a function of time and relative position of the scattering cloud and the compact source of continuum radiation. Time evolution assumes short flare of continuum emission. The time tags marked in the left column indicate the time elapsed since the moment, when the surface of the illuminating parabola touched the cloud for the first time (see text and Fig.2). The intensity of the the primary source was adjusted for each column in order to have the same total flux from the cloud for row marked as ‘30’(years). The position of the cloud with respect to the source is indicated with a pair of numbers at the bottom of the figure. The topmost row of images corresponds to the moment of time when the surface of the parabola goes through the centre of the cloud. Density distribution in the cloud adopted from Lis and Goldsmith, 1989 (see equation (7)). **Right:** The same as in the left figure, but for the 100 times less dense cloud – i.e. in the limit of optically thin cloud. Note that in this limit surface brightness at any given moment of time reflects the density distribution over the surface of the parabola.

3.1.4 Surface brightness distribution (short flare)

The Fig.3 shows similar time evolution of the surface brightness for the case of a very short flare of the primary source. Note that for an optically thin case (Fig.3) surface brightness distribution reflects the density distribution in the cloud along the surface of the parabola. For the thicker cloud (Fig.3) photoabsorption may eliminate peaks associated with denser condensations and even produce ‘holes’ at their positions and cast ‘shadows’ on the more distant (from the primary source) parts of the cloud. The temporal behavior of the surface brightness distribution towards the centre of the cloud is shown in Fig.4. Different curves corresponds to the different normalizations of the density distribution in the cloud. For optically thin cloud time evolution simply characterizes the density structure of the cloud along the line of sight. For the thicker cloud photoabsorption naturally limits the possibility to probe inner regions of the cloud.

3.1.5 Time evolution of the flux from the whole cloud (short flare)

. The evolution of the total flux from the cloud (for the case of very short flare) is shown in Fig.5. The position of the cloud with respect to the source (x, z) is marked in each plot in units of cloud radius r . Time is measured in units r/c . Bottom row correspond to the case of the source, which pro-

jected position coincides with the cloud centre. Upper two rows correspond to the cloud which is shifted (in projection) by 3 and 6 cloud radii from the source position. The relative distance of the source and the cloud vary for the plots in different columns. The leftmost column correspond to the cloud which is closer to the observer than the source by 8 cloud radii. The rightmost column correspond to the cloud which is further away than the source by 8 cloud radii. One can see that duration of scattered flare strongly depends on the position of the cloud with respect to the primary source. This compensates to some extent the drop of the maximal flux with distance (due to decrease of the solid angle) for the clouds located closer to the observer than the source. The maximal flux drops with distance along Z coordinate as $1/z$ for such clouds, compared to $1/z^2$ dependence for clouds more distant, than the source.

Note that there are three factors limiting the time scale and the amplitude of 6.4 keV flux variability from a given direction. First of all the shortest possible time scale Δt (and amplitude) are defined by the variability of the primary source. The second factor is nonuniformity of the matter distribution on the spatial scales corresponding to the ‘thickness’ of the parabola (which is $0.5\Delta tc(1 + \eta^2)$). The third factor is the velocity of the parabola motion with respect to the spatial nonuniformities of the neutral matter.

Finally one can note that although the flux of the 6.4 keV line may vary by orders of magnitude depending on the

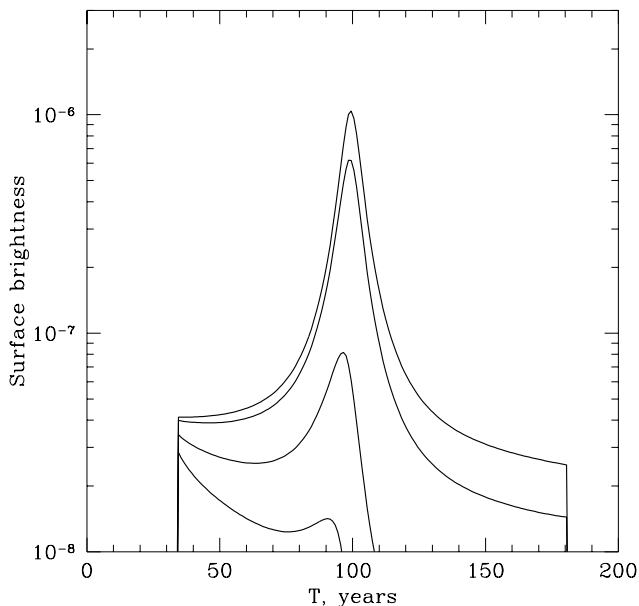


Figure 4. Time evolution of the surface brightness of the cloud towards the centre. The shape of the density distribution is the same for all curves, but normalizations are different. The lowest curve corresponds to the Lis and Goldsmith (1989) model of the Sgr B2 cloud. The other curves (from bottom to top) correspond to the cloud with density scaled by factors of 0.5, 0.1 and 0.01 with respect to the Lis and Goldsmith model. The flux of the source was scaled inversely to this factor in order to keep the same intensity of the scattered flux assuming optically thin regime. The primary source was assumed to be located at the same distance as the cloud, but 100 pc away from the cloud in the picture plane.

geometry of the cloud and its relative position with respect to the source the equivalent width should be approximately constant, since continuum is scattered in a similar way. The equivalent width may vary however by a factor of ~ 2 , due to the difference of isotropic indicatrix (line) and dipole indicatrix (Thomson scattered continuum). The largest equivalent width is expected for the cloud which is located at the same distance as the source, but is shifted from the source in the picture plane such that ~ 90 degree scattered photons are dominating continuum. Variations of equivalent width due to this effect are clearly seen in Fig.7 below.

In the light of the above discussion one can rise the question why the Sgr B2 is brighter in the 6.4 keV line than other molecular clouds in the region if Sgr A* is a source of primary radiation. One can consider following possibilities:

I The parameters of the Sgr B2 cloud (Thomson optical depth, solid angle occupied by the cloud as seen from the Sgr A* position) may be favorable for high output in terms of the 6.4 keV line flux. If one starts with the cloud of very low optical Thomson depth τ_T , then the flux in the line will be simply proportional to τ_T . With increase of τ_T the photoabsorption effects start to be important and in the limit of very thick cloud most of the radiation will be absorbed (unless the side of the cloud towards observer is illuminated). Optimal for the formation of the iron fluorescent line is the

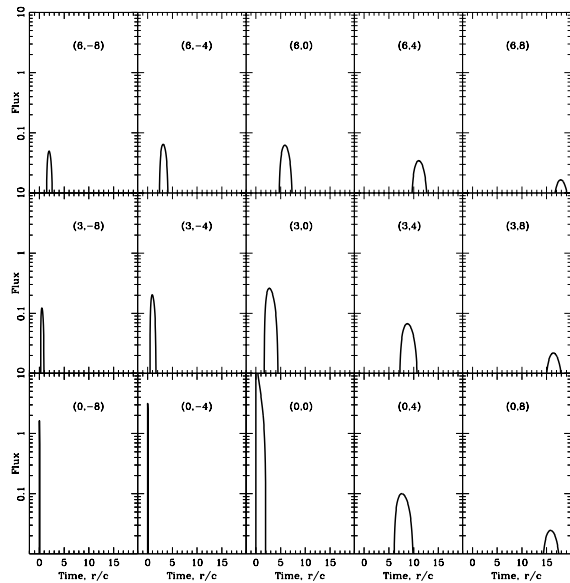


Figure 5. Total flux from the cloud versus time for different mutual locations of the source and the cloud. The duration of the flare was assumed to be much shorter than the light crossing time of the cloud. The positions indicated are measured in cloud radii. The time is measured in units of light crossing time of the cloud.

Thomson depth $\tau_T \sim 0.4$. This value roughly corresponds to the Thomson optical depth of the Sgr B2 cloud. Thus we conclude that at least partially brightness of the Sgr B2 cloud can be attributed to the ‘optimal’ optical depth of the cloud. If the clouds have considerable optical depth then their brightness in the 6.4 keV will strongly depend on what side of the cloud is illuminated (seen by observer or an opposite one).

II The intense primary radiation may be due to a relatively short episode of efficient accretion onto Sgr A* few hundreds years ago and Sgr B2 cloud is located ‘at the right place’ (see Fig.1) such that light propagation time from Sgr A* to the cloud and then to the observer compensates the time delay. In other words only selected clouds (e.g. Sgr B2, Radio Arc region) are exposed to the primary radiation from Sgr A* at ‘present’ time. Other clouds in this region either will be bright in future or primary radiation already left them.

III The emission from Sgr A* may be anisotropic, e.g. due to the blocking by dust at some directions (Koyama et al. 1996), or intrinsically collimated (e.g. jet) and pointed towards Sgr B2.

Further imaging observations of the Galactic Centre region in the 6.4 keV line may reveal many smaller clouds, which trace the volume occupied by the radiation from the putative transient source.

3.1.6 Long Duration Flare

In the case of the illumination front broader than the dimension of the molecular cloud ($c\Delta t > r_{cloud}$) the K_α line surface brightness is proportional to the optical depth of the cloud (in the limit of small τ_T) and the total K_α flux is proportional to the mass of molecular hydrogen inside the cloud (see Sunyaev et al., 1993).

3.2 Multiple scattering problem

Even when the primary photons have already left the cloud, multiply scattered photons can be observed. Indeed, part of the 6.4 keV photons produced due to absorption of primary continuum radiation will be Thomson scattered and will leave the cloud with some delay with the respect to the primary radiation. This delay can be of the order of light crossing time of the cloud. This is especially important for clouds located between the compact source and observer, since primary radiation may leave such clouds on a time scales much shorter than light crossing time of the cloud. The flux of the radiation leaving the cloud with significant delay should be small – for Thomson depth much less than unity most of the photons leave the cloud without scattering, while for large Thomson depth the photoabsorption will significantly attenuate the flux. However, given the present day line flux from the Sgr B2 cloud (few 10^{-4} $phot\ s^{-1}cm^{-2}$, Koyama et al., 1996) it is clear that even 100-1000 times weaker flux can be easily detected by future missions like *Constellation* or *Xeus*. The time dependence and the shape of the multiply scattered line is considered in the next section.

4 EQUIVALENT WIDTH

The case of the source located outside the cloud and illuminating the side of the cloud towards the observer was intensively discussed in the literature in application to the spectra reflected by the surface of accretion disk or dust torus in AGNs (see e.g. Matt et al. 1991, Awaki et al. 1991, Nandra & George 1994, Ghisellini et al. 1994). We concentrate below on the simple model of a source embedded into the neutral gas cloud and consider time evolution of the equivalent width and the shape of the line.

One of the most important parameters determining the possibility of the line detection is its equivalent width (EW), i.e. the ratio of the flux in the line to the spectral density of the continuum flux at the same energy. We use Monte-Carlo simulations in order to generate spectra, emerging from a spherically symmetric cloud with uniform density and a point source of the continuum radiation (power law with photon index $\Gamma = 1.8$) in the centre. Initial seed photons were generated in the 1–18 keV energy range. Since temporal behavior of the 6.4 keV line flux is in question we kept record of escape time for photons, emerging from the cloud. Shown in Fig.6 is the evolution of the line and continuum fluxes with time for the case of short flare at $t = 0$ (upper row of figures) and theta-function-like behavior of primary source flux (lower row of figures). In the latter case the flux of the source was stable before the moment of time $t = 0$ and dropped to zero level after this moment. In both

cases $t = 1$ corresponds to the moment of time, when direct radiation (towards observer) leaves the cloud. Three values of the cloud radial Thomson depths $\tau_T = 0.01$ (a), 0.2 (b) and 0.5 (c) were used. In Fig.7 the evolution of the equivalent width of the 6.4 keV line is shown for the same set of parameters. The thin solid line shows the contribution of the 6.4 keV photons, which left the cloud without further interactions. The dotted line shows the contribution of the 6.4 keV photons which have been Thomson scattered once and the dashed line shows the 6.4 keV photons which undergo more than one scattering before they escaped from the cloud. At last thick solid line shows total contribution of all these components. Note that scattered 6.4 keV photons may have an actual energy lower than 6.4 keV (we discuss the shape of the line profile below).

The first thing apparent from Fig.7 is the sharp change of EW at the $t = 1$. This is obviously related to the disappearance of the direct component (escaping from the cloud without interaction), which contributes to the continuum emission. Immediately after $t = 1$ EW jumps to the level of ~ 1 keV for all three values of τ_T (Fig.7 a,b,c). Indeed (see e.g. Vainshtein & Sunyaev, 1980) both flux in the line and the level of the scattered continuum emission are (to the first order) proportional to the amount of matter over the radius of the cloud. As the results, the EW (ratio of the line flux to the continuum spectral density) happens to depend only weakly on the actual parameters of the cloud.

Note also (see Fig.7a) the specific (curved) shape of the EW behavior in the period of time $t = [1, 3]$, when single scattered continuum photons and unscattered 6.4 keV photons dominate the spectrum. This shape (a deviation from the constant level) is due to the difference in the angular distribution of the scattered continuum photons and those in the 6.4 keV line. Indeed 6.4 keV photons are emitted by iron atoms isotropically, while continuum photons, scattered by electrons, follow Rayleigh (dipole) indicatrix $\frac{d\sigma}{d\Omega} \propto (1 + \cos^2\vartheta)$. A difference in the escape time for continuum and line photons causes this specific shape.

However for large values of optical depth (Fig.7c) the behavior of the EW is very different – its value starts to rise from early beginning. One of the reasons for such a behavior is a significant photoabsorption depth. Continuum photons (at about 6 keV) have a high probability to be absorbed before they can escape from the cloud. On the other hand high energy photons (at the energy 10–20–30 keV) can reach peripheral regions of the cloud without being absorbed, ionize an electron from the iron K-shell and thus produce a 6.4 keV photon, which can escape further. One can get an idea of how the EW depends on the depth of the scattering region from Fig.8. The following function $Y \cdot \delta_{Fe} \int_{7.1keV}^{\infty} \frac{I(E) \exp(-\sigma_{ph}(E)\tau_T/\sigma_T) \sigma_{Fe}(E) dE}{I(E_0) \exp(-\sigma_{ph}(E_0)\tau_T/\sigma_T)}$ is plotted here versus the optical depth τ_T . This function characterizes how the equivalent width of the line in the scattered component changes if the primary radiation has passed through the absorbing matter before the scattering place. Absorption just modifies the shape of the spectrum, suppressing continuum at ~ 6 keV stronger than at energies above ~ 10 keV. As a result one can expect that for large values of the optical depth the EW of the line in the scattered component will be larger than that in the case of small τ_T .

Even apart from the photoabsorption effect the total

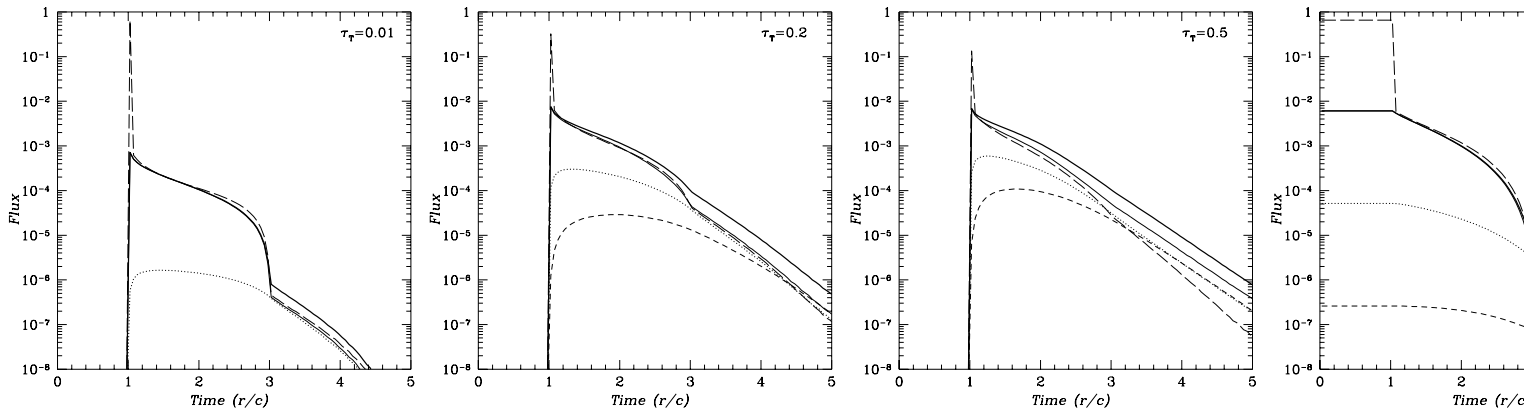


Figure 6. Flux versus time for the compact source of continuum emission at the centre of the uniform spherical cloud. The upper row of figures corresponds to the short flare of the compact source flux, the lower row of figures corresponds to the ‘switch-off’ of the steady source. In both cases the propagation time from the centre of the cloud to the outer edge was taken into account. Thus flare at the centre of the cloud at $t = 0$ appears as a spike at $t/(r/c) = 1$ in the figures. The thin solid line shows the contribution of the 6.4 keV photons, which left the cloud without further interaction. The dotted line shows the contribution of 6.4 keV photons which have been Thomson scattered once and dashed line shows the 6.4 keV photons which undergo more than one scattering before escaping from the cloud. The thick solid line shows total contribution of all these components. At last long-dash line shows the continuum flux (in the energy range [5.9–6.9] keV). Time is expressed in units of light crossing time of the cloud (radius divided by speed of light).

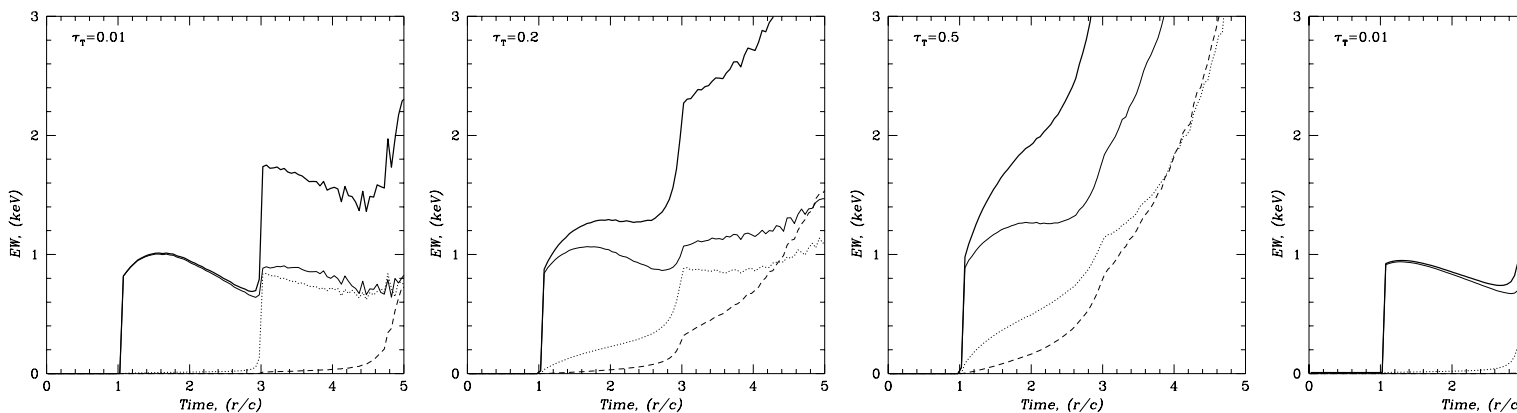


Figure 7. The equivalent width versus time for the compact source of continuum emission at the centre of the uniform spherical cloud. The upper row of figures corresponds to the short flare of the compact source flux, the lower row of figures corresponds to the ‘switch-off’ of the steady source. The thin solid line shows the contribution of the 6.4 keV photons, which left the cloud without further interactions. The dotted line shows the contribution of 6.4 keV photons which have been Thomson scattered once and dashed line shows the 6.4 keV photons which undergo more than one scattering before escape from the cloud. The thick solid line shows total contribution of all these components.

EW calculated as the sum of unscattered and scattered 6.4 keV photons (Fig.7 a,b,c) grows with time. For low values of optical depth this growth is seen as the sharp jump at $t = 3R/c$. This jump corresponds to the moment when all photons, which undergo only one interaction (absorption + fluorescence or single Thomson scattering) are leaving the cloud. After that moment of time the spectrum is dominated by the photons passed through more than one interaction. One can see that the EW of the 6.4 keV complex increases at that moment. This is because continuum is now dominated by twice Thomson scattered photons, while the line is constructed from two kinds of photons: (a) photons which first

were Thomson scattered, then ionized an electron from iron K-shell and produced new 6.4 keV photon and (b) Thomson scattered 6.4 keV photons. The EW for each of these components (with respect to twice Thomson scattered continuum photons) is about 1 keV. After each additional scattering (when the spectrum is dominated by the photons passed through n interactions) the total equivalent width will increase further (roughly proportional to n). In other words one can say that with each additional ‘interaction’ Thomson scattering does not change the existing EW of the line, while ionization of iron K-shells adds more ‘fresh’ 6.4 keV photons.

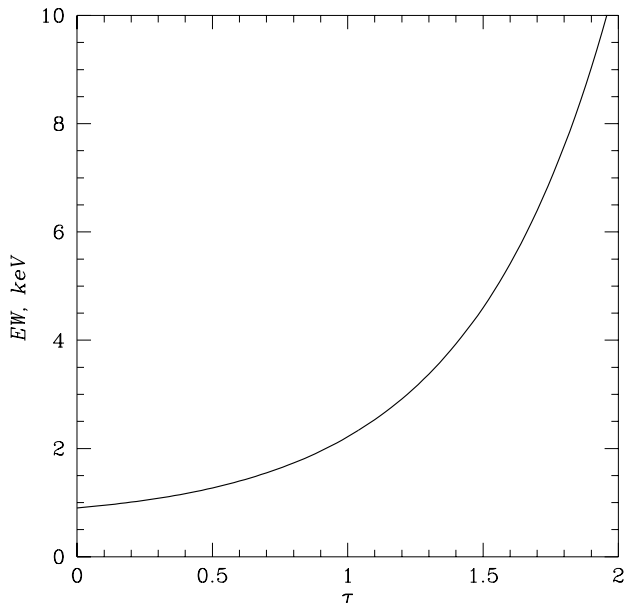


Figure 8. Dependence of the equivalent width on the optical depth of the media. The photons at ~ 6 keV have a higher probability as being absorbed, compared to high energy photons (10–20 keV), which can pass through larger depth and cause emission of the 6.4 keV photons. One can expect to find such an equivalent width in the scattered component if the radiation has passed through the absorbing matter with the optical depth τ_T before entering the region from which reprocess radiation is observed.

Finally one can note that although the EW of the 6.4 keV complex rises with time absolute flux declines with time (Fig.6). The decline of the flux is caused by the escape of the photons from the cloud and photoabsorption of photons. The fraction of photons which can be detected after additional light crossing time of the cloud is less than $\sim \tau_T e^{-\tau_T \sigma_{ph}(E)/\sigma_T}$. This factor reaches maximum (~ 0.14) at Thomson depth of the cloud $\tau_T \sim 0.4$. Note that for the Sgr B2 complex ASCA detected the 6.4 keV flux at the level of few $10^{-4} phot s^{-1} cm^{-2}$ (Koyama et al. 1996) and even a 1000 times weaker line will still give a few hundred counts for 100 msec observation with the *Constellation* mission. It means that in principle with *Constellation* it may be possible to detect traces of the 6.4 keV emission even if the time elapsed since the initial flare exceeds the light crossing time of the cloud by a factor of few. In order to multiple scattered photons dominate the spectrum the cloud has to have rather sharp boundary. As noted above although the life time of the n -times scattered photons is longer than for photons which undergo $n - 1$ scatterings, the flux decreases by a factor of at least 0.14 (and in fact more, see Fig.6) with each additional scattering. If a very extended envelope (with weakly declining density) of the cloud is present or if the primary continuum flux was declining too slowly, then fluorescent photons generated by primary radiation may dominate the total spectrum of the cloud. However in the presence of optically thick blobs immersed into more tenuous phase they may effectively screen more distant layers of the cloud

(which are still exposed to primary radiation) while their surface seen by the observer will reflect 6.4 keV photons.

5 SHAPE OF THE LINE

In the previous section the fact that photons can change their energy during scattering was not taken into account. However for the 6.4 keV photons even single scattering causes significant change of energy, which is especially important for future instruments with high energy resolution. Since we are considering scattering by the neutral matter, then all complications related to bound electrons (discussed in Sunyaev & Churazov, 1996) are to be taken into account. Although we are considering molecular cloud, for simplicity we used below analytical formulae for scattering by hydrogen atoms. Compton scattering (affected by momentum distribution of the electron) should be very similar for atomic and molecular hydrogen.

For the 6.4 keV photons after each scattering (by a hydrogen atom) about 14 per cent of the photons will maintain the initial energy unchanged (Rayleigh or elastic scattering). For molecular hydrogen this value is higher due to the coherent scattering by two electrons. Some small fraction photons will cause excitation of electrons in the hydrogen atoms, leading to the appearance of Raman satellites of the line at the energies $h\nu_0 - 13.6 \times (1 - 1/n^2)$ eV, where n is the principle quantum number of excited level. But the largest fraction of photons will be Compton scattered by hydrogen atoms, leading to the ionization of an electron and decrease of the photon energy by ~ 13 –200 eV. Due to the motion of the electrons bound in hydrogen atoms, the backscattering peak will be smeared out.

Shown in Fig.9 are the spectra, emerging from the spherical cloud (with the radial optical depths of 0.2) after a given time from the switch-off of the compact source. We assume here that fluorescence produces a monochromatic line at the energy of 6.4 keV. One can see that after multiple scatterings a complex shoulder forms on the low energy side of the line. As discussed above the total equivalent width of the whole complex increases with time. However the photons are now distributed over a rather broad energy range, which increases with time. The equivalent width of the unshifted 6.4 keV line itself will still increase with time. This is related in part with the more rapid decline of the continuum at 6.4 keV due to photoabsorption (see above) and in part with Rayleigh scattering, which leaves ~ 14 per cent of the photons at the initial energy (see also below).

6 ABSORPTION EDGE

High sensitivity and energy resolution of the coming missions will be sufficient to study the absorption edge (at 7.1 keV) in much more details. Shown in Fig.10 is the evolution of the absorption edge structure for the similar sets of moments of time as in Fig.9. Since the feature is intrinsically broad we ignored the complications associated with scatterings by bound electrons and used standard formulae for recoil effect on the free electrons in order to study evolution of the shape of the spectrum. Multiple scattering cause shift of the feature to lower energies and smearing of the edge

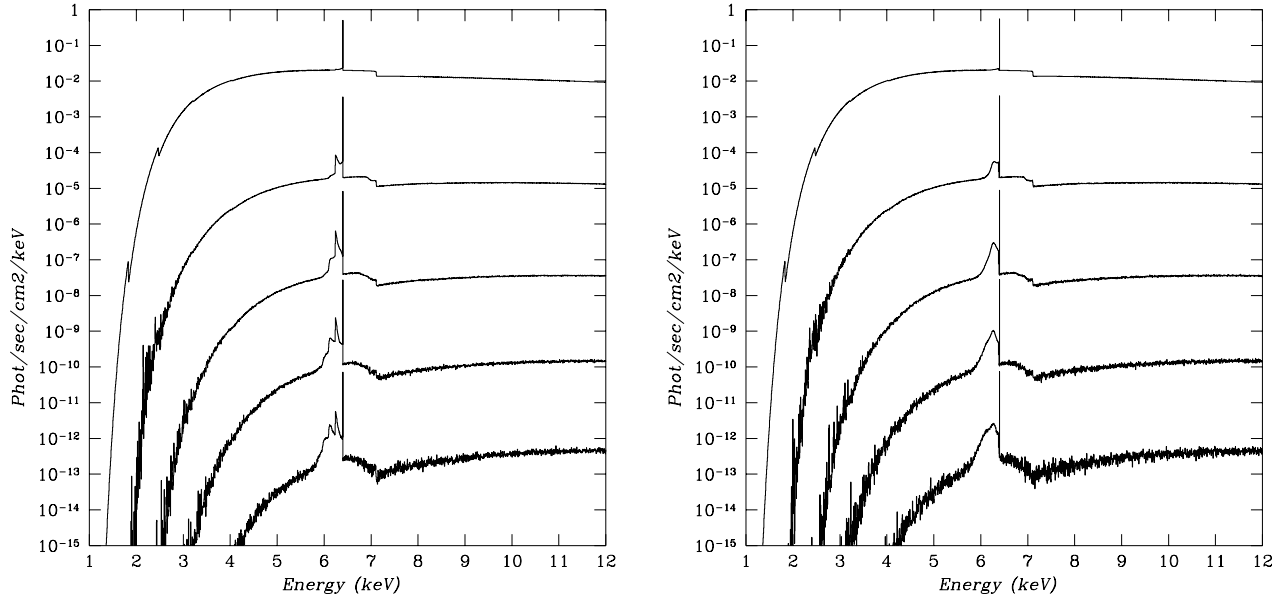


Figure 9. Spectra emerging from the uniform cloud with radial Thomson depth $\tau_T = 0.2$ at different moments of time after a short flare of the continuum emission from the point source in the centre of the cloud. For the left figure the recoil effect was calculated as for free cold electrons at rest. For the right figure effects of bound electrons were taken into account (but only for the 6.4 keV line). Spectra correspond to the intervals of time: 0–1, 1–2, 2–3, 3–4, 4–5 (in units R/c). Each subsequent spectrum was multiplied by 0.05 for clarity. Spectra are plotted with an energy resolution of 5 eV.

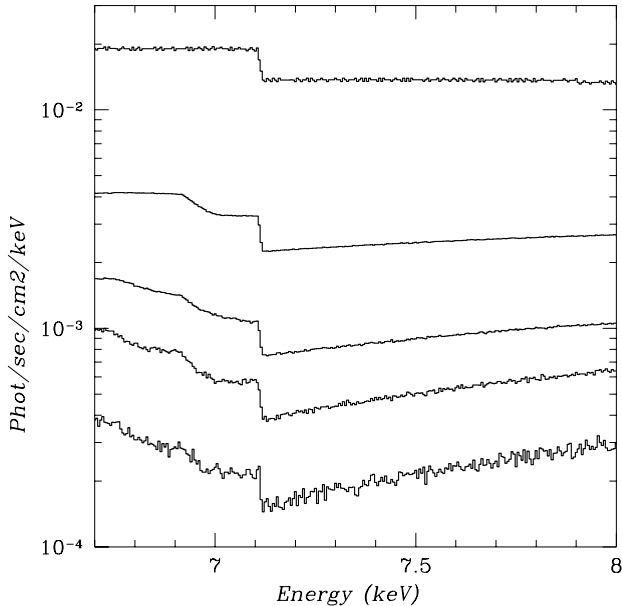


Figure 10. Evolution of the iron absorption K-edge with time. Spectra correspond to the intervals of time: 0–1, 1–2, 2–3, 3–4, 4–5 (in units R/c). Each subsequent spectrum was multiplied by a factor of 10.

structure. Sharp jump at 7.1 keV has always the same relative amplitude, which simply reflects the absorption depth after the last scattering.

For the case of a steady source inside a cloud the observed flux in the 6.4 keV line is uniquely related to the observed deficit of photons above K-edge. The coefficient relating these two quantities is simply the fluorescent yield $Y \approx 0.3$. In other words equivalent width of the line is approximately factor of 3 smaller than effective equivalent width of the absorption edge. For the reprocessed radiation (i.e. when primary source is not visible) this relation may break. This is clear considering e.g. the case of the cloud of extremely low optical depth. Indeed as one can see from Fig.7 (left column) equivalent width emerging from an optically thin cloud can be high. On the other hand observed deficit around 7.1 keV (even if we integrate it with account of smeared absorption structure) can be very small for low values of optical depth of the cloud.

7 COMPLEX GEOMETRIES

Of course in the case of more complex geometries (e.g. extended envelopes) and complex time history of the primary radiation flux the whole picture will be accordingly much more complex. However some general properties (which are demonstrated with the above simple models) may be used to get an idea of the what we can look for with future X-ray observations of the Galactic Centre region in order to understand the origin of the fluorescent line.

The high sensitivity and high angular resolution map-

ping of this region in the 6.4 keV may reveal a number of small clouds (along with more detailed structure of the Sgr B2 cloud and Radio Arc region) which are tracing the volume occupied by primary radiation of putative flare of the Sgr A*. Morphology of the line surface brightness distribution may help to determine the location of the primary source. Broad band spectra of these clouds may also provide an information on the primary source location, since low energy absorption depends crucially on the side from which the cloud is illuminated. Indeed, if the side of the cloud towards observer is illuminated by a primary source, then instead of exponential cutoff at low energies due to photoabsorption (as in the case of the cloud illuminated from the back) one can expect much shallower decline.

For some clouds inspite of the low absolute flux the equivalent width of the line can be in excess of 1 keV due to photoabsorption effects or multiple scatterings*. Narrow line and sharp absorption edge at 7.1 keV can be considered as the indicators of strong photoabsorption, while the complex shape of the line (extended left wing) and smeared absorption edge indicate that multiple scatterings are dominant.

Important results can be obtained studying dense condensations which are optically thick. Since they screen the more distant layers of the gas one can use them as indicators of the position of surface which separates regions filled with primary photons from 'empty' regions. From such condensations scattered 6.4 keV line may be detected even if the cloud has extended envelope.

Principle information can be obtained comparing the data which were obtained at different moments of time (separated by ~ 5 years). Detection of changes in the surface brightness, equivalent width and shape of the 6.4 keV would provide exciting and unique insight on the time history of the putative supermassive black hole at the Centre of our Galaxy.

8 CONCLUSIONS

The value of the equivalent width and the shape of the 6.4 keV iron K_{α} line, emerging from the neutral matter, illuminated from inside or outside by the X-ray continuum spectrum, contains information on the time history of the illuminating continuum flux. Assuming normal abundance of iron in the scattering media the value of an equivalent width of about 1 keV indicate that we are dealing with a scattered component. Values in excess of 1 keV can be due to strong photoabsorption or multiple Thomson scattering. Spectroscopic analysis of the 6.4 keV line profile and the shape of the 7.1 keV absorption edge can help to distinguish between these possibilities. When combined with broad band spectroscopic measurements it can be used to determine the position and flux history of the primary continuum source. A new generation of X-ray instruments should be capable

* Of course, the extended emission due to the hot gas in the Galactic Centre region may actually dominate the continuum at 6.4 keV causing the decrease of the observed equivalent width. However one can estimate it's contribution using the intensities of the strongly ionized iron emission lines, in particularly at ~ 6.7 keV.

of achieving the required sensitivity and energy resolution to accurately measure the detailed structure of the 6.4 keV line in the Galactic Centre region. Comparing the flux and shape of the line from different molecular clouds in the region, one can reconstruct the date and duration of the flare, responsible for observed reprocessed emission. Note also that observations, over a period of 5–10 years, may show the variability of the line flux, shape and morphology of it's surface brightness distribution.

The assumption that Sgr A* emission has caused the 6.4 keV line (and continuum) emission from Sgr B2 (Sunyaev et al. 1993; Koyama et al. 1996) implies that its flux vary by a factor of at least 10^3 (and perhaps much more) on a time scale of hundreds of years. If nuclei in other galaxies also have similar behavior there is a good chance of detecting 'delayed' scattered components from some of them. With the high sensitivity of the *Constellation* mission one can search for very weak nearby and distant AGNs. The detection of an iron line of large equivalent width and complex shape would prove the past violent activity of the central engines of these sources.

This work was supported in part by the grants RBRF 96-02-18588 and INTAS 93-3364-ext. We thank Marat Gilfanov for useful discussions and anonymous referee for helpful comments.

REFERENCES

- Awaki H., Koyama K., Inoue H., Halpern J.P., 1991, PASJ, 43, 195
 Bambinek W. et al. 1972, Rev. of Modern. Phys., 44, 716
 Basko M. 1978, ApJ, 223, 268
 Basko M., Sunyaev R., Titarchuk L., 1974, A&A, 31, 249
 Beckert T., Duschl W.J., Mezger P.G., Zylka R., 1996, A&A, 307, 450
 Chevalier R., 1986, ApJ, 308, 225
 Churazov E., Gilfanov M., Sunyaev R., 1996, ApJ, 464, L71
 Fabian A.C., 1977, Nature, 269, 672
 Hasegawa T., Sato F., Whiteoak J., Miyawaki R., 1994, ApJ, 429, L77
 George I.M. & Fabian A.C., 1991, MNRAS, 249, 352
 Genzel R., Hollenbach D., Townes C., 1994, Rep. Prog. Phys., 57, 417
 Gilfanov M., Sunyaev R., Churazov E., 1987, Soviet Ast. Letters, 13, 233
 Gilfanov M., Sunyaev R., 1998, in preparation
 Ghisellini G., Haardt F., Matt G., 1994, MNRAS, 267, 743
 Illarionov A., Kallman T., McCray R., Ross R., 1979, ApJ, 228, 279
 Inoue H., 1985, Space Sci. Rev., 40, 317
 Katz J.L, 1987, A&A, 182, L19
 Koyama K, 1994, New Horizon of X-ray Astronomy, FSS-12, 181, Univ. Acad. Press, Tokyo
 Koyama K., Maeda Y., Sonobe T., Takeshima T, Tanaka Y., Yamauchi S., 1996, Publ. Astron. Soc. Japan, 48, 249
 Lis D.C., Goldsmith P.F., 1989, ApJ, 337, 704
 Markevitch M, Sunyaev R., Pavlinsky, 1993, Nature, 364, 40
 Matt G., Perola G.C., Piro L., 1991, A&A, 247, 25
 Menten K.M, Reid M.J., Eckart A., Genzel R., 1997, ApJ, 475, L111
 Milgrom M., 1987, A&A, 182, L21
 Morrison R., McCammon D., 1983, ApJ, 270, 119
 Nandra K., George I.M., 1994, MNRAS, 267, 974
 Rees M.J., 1988, Nature, 333, 523

- Pavlinisky M., Grebenev S., Sunyaev R., 1994, ApJ, 425, 110
 Predehl P., Trümper J., 1994, A&A, 290, L29
 Rieke G.H., Rieke M.J., Paul A.E., 1989, ApJ, 336, 752
 Stark A.A., Gerhard O.E., Binney J., Bally J., 1991 MNRAS, 248, 14p
 Sunyaev R., Markevitch M., Pavlinisky M., 1993, ApJ, 407, 606
 Sunyaev R., Churazov E., 1996, Astronomy Letters, 22, 648
 Turner M.J.L., et al., 1997, The Next Generation of X-ray Observatories: Workshop Proceedings, M.J.L. Turner & M.G. Watson, eds., Leicester X-ray Astronomy Group Special Report, XRA97/02, p.165
 Tanaka Y., Shibazaki N., 1996, Annual Review of Astronomy and Astrophysics, 34, 607.
 Vainshtein L., Sunyaev R., 1980, Soviet Ast. Letters, 6, 673
 Vainshtein L., Sunyaev R., Churazov E., 1998, Astronomy Letters, (in press).
 de Vicente P., Martin-Pintado J., Wilson T.L., 1997, A&A, 320, 957
 Wise M.W., Sarazin C.L., 1992, ApJ, 395, 387
 White N.E., Tananbaum H., Kahn S.M., 1997, The Next Generation of X-ray Observatories: Workshop Proceedings, M.J.L. Turner & M.G. Watson, eds., Leicester X-ray Astronomy Group Special Report, XRA97/02, p.173

APPENDIX A: SIMPLIFIED TREATMENT

An exact account for complex geometry, scattering diagram and photoabsorption effects make the Monte–Carlo method most suitable for solving each particular problem. However all major effects can be easily seen from the simplified treatment, given below.

A1 Equivalent Width

Let us consider the evolution of spectrum for the short flare of continuum emission in a cloud of Thomson (and photoabsorption) depth $\tau_T \ll 1$. One can construct a ‘toy’ model assuming that fraction of photons $\sim \tau_T$, which undergo additional scattering, will leave the cloud with time delay T . Therefore intensity of the continuum (at 6.4 keV and above iron K–edge) at a given moment of time t can be written as follows:

$$N_c^{6.4}(t) = N_c^{6.4}(t - T) \cdot \tau_T \quad (\text{A1})$$

$$N_c^{7.1}(t) = N_c^{7.1}(t - T) \cdot \tau_T \quad (\text{A2})$$

We further assume that similar delay T is applicable to the continuum photons, which have been absorbed by iron K shell and reemitted as 6.4 keV photons. Therefore:

$$N_l^{6.4}(t) = N_l^{6.4}(t - T) \cdot \tau_T + N_c^{7.1}(t - T) \cdot \tau_T Y \delta_{Fe} \frac{\sigma_{Fe}}{\sigma_T} \quad (\text{A3})$$

First term in the right side of equation (A3) corresponds to scattering of existing 6.4 keV photons, while the second term describes generation of new 6.4 keV photons. Dividing equation (A3) by the equation (A1) one gets an expression for the equivalent width of the line:

$$EW(t) = EW(t - T) + \frac{N_c^{7.1}(t - T)}{N_c^{6.4}(t - T)} \cdot Y \delta_{Fe} \frac{\sigma_{Fe}}{\sigma_T} \quad (\text{A4})$$

The last term in the equation (A4) does not depend on time or Thomson depth and its numerical value is ~ 1 keV (see previous sections). Thus from equation (A4) it is clear that

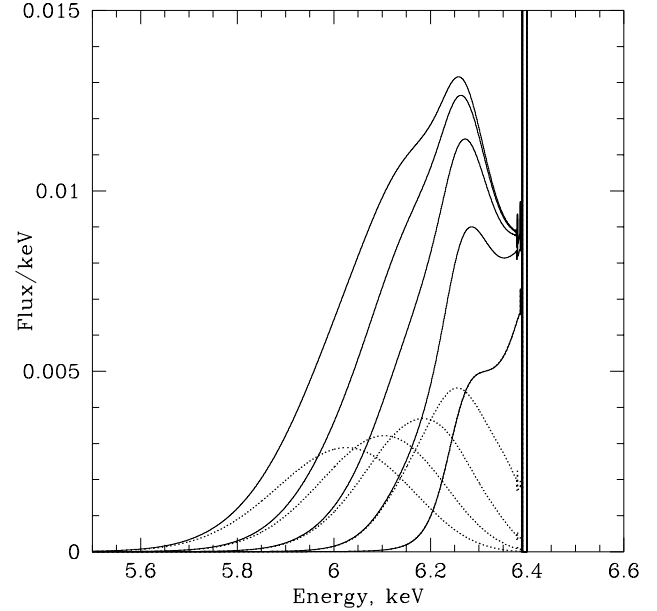


Figure A1. Shape of the line after the period of time $\frac{t}{R/c} = 1, 2, 3, 4, 5$ since short flare of continuum emission (simplified treatment, see text). The dotted lines show the spectra of a monochromatic line after 1, 2, 3, 4, 5 scatterings.

equivalent width rises by ~ 1 keV with each additional time interval T .

$$EW(t) = EW(t - T) + 1 \text{ keV} \quad (\text{A5})$$

Account for photoabsorption causes additional increase of the equivalent width with time.

A2 Shape of the line

Considering again the case of $\tau_T \ll 1$ and neglecting the correlation of the escape probability with scattering angle one can calculate the spectrum of the 6.4 keV line complex after $t = nR/c$. This spectrum can be represented as the sum of spectra $\sum_1^n F_n(E)$, each having the same flux. $F_1(E)$ is the ‘fresh’ 6.4 keV line, which will be treated below as monochromatic, each F_{i+1} can be derived from F_i , convolving F_i with the differential cross section of scattering, averaged over all angles. Using the differential cross section for a hydrogen atom (e.g. Sunyaev & Churazov, 1996) one can get the sequence of spectra shown in Fig.A1 (cf. Fig.1 in Illarionov et al., 1979 for the case of scatterings on the cold free electrons). Dotted lines show individual F_i spectra, while solid lines show sums of F_i for $n = 1, 2, 3, 4, 5$. As noted above, the total flux of the line will strongly decline with time, but high equivalent width will, on the contrary, rise, which may help to detect and resolve the shape of the line even if the absolute flux is low. One can see that the shape of the feature closely resembles the one obtained from Monte–Carlo calculations (Fig.9), although quantitatively they may differ (e.g. because of the correlation of the escape probability with scattering angle). In particular this correlation may be important for the contribution to the intensity of the unshifted

6.4 keV line due to Rayleigh scattering, which corresponds to small scattering angles. In the simplified treatment (as above) the width of the line after n scatterings is equal to $\approx 1 + (0.14) + \dots (0.14)^n$, where the factor ~ 0.14 is the probability of Rayleigh scattering for the ~ 6.4 keV photons, averaged over all scattering angles. In reality the intensity of this line will be lower, since photons, scattered by small angle continue to move towards edges of scattering media. For molecular hydrogen (which is of course the dominant part of the cloud) due to coherent scattering the fraction of elastic scatterings (as well as total scattering cross section) will be higher. Helium atoms also contribute significantly to the coherent scattering (Vainshtein, Sunyaev & Churazov, 1998). However elastic scattering dominates at rather small scattering angles thus reducing the impact of enhanced elastic scattering onto observed spectra. Monte-Carlo simulations of the particular geometry of the scattering cloud are required to calculate the actual fraction of unshifted 6.4 keV line in the observed spectrum.